A new algorithm for near–singular integration of 3D Boundary Element Integrals for thin–walled elements

Un nuevo algoritmo para la integración cuasi-singular en el Método de Elementos de Contorno tridimensional aplicado a elementos de pared delgada

Marco Antonio González de León[1], Luiz Carlos Wrobel[2], Manuel del Jesús-Martinez[3]*

[1] Departamento de Mecánica, Universidad Simón Bolívar. Sartenejas, Baruta, Estado Miranda. Apartado 89000. Caracas, Venezuela.

[2] Institute of Materials and Manufacturing, Brunel University London. Kingston Lane, Uxbridge. Middlesex UB8 3PH. Uxbridge, UK.

[3] Escuela de Ingeniería Mecánica, Facultad de Ingeniería, Universidad Central de Venezuela. Ciudad Universitaria, Los Chaguaramos. Apartado Postal 48222. Caracas, Venezuela.

(Received December 13, 2013; accepted September 19, 2014)

Abstract

The accuracy of the Boundary Element Method (BEM) is strongly dependent on an accurate evaluation of boundary integrals. For thin-walled structures, collocation points and integration elements are often very close, making the kernel of the integrations nearly singular and requiring the use of special numerical integration techniques. In this paper, an effective algorithm is presented for near–singular integration of boundary element integrals applied to three–dimensional thin-walled structures. A combination of Telles' transformation of variables technique and an adaptive Gaussian quadrature method for regular integrals is used to improve the integration accuracy and to decrease the computation time. The choice of parameters for the technique depends on the relationship between the distance from collocation point to integration element and a reference element length. The proposed integration algorithm is applied to thin plate uniaxial loading and pressurized thin-walled cylindrical shells. The results obtained are in good agreement with theoretical results and the reduction in integration times is significant.

* Corresponding author: Marco Antonio González de León, e-mail: margdleon@usb.ve

----------*Keywords:* BEM, plates, shells, numerical integration, polynomial transformation

Resumen

La exactitud del Método de Elementos de Contorno (MEC) depende fuertemente de una evaluación precisa de las integrales de contorno. En estructuras de pared delgada, algunos puntos de colocación pueden estar muy cerca de elementos de integración, generando integrales cuasi-singulares que requieren el uso de técnicas especiales de integración numérica. En este trabajo, se presenta un algoritmo efectivo para la integración cuasi-singular en el MEC aplicado a estructuras de pared delgada en tres dimensiones. El algoritmo se basa en una combinación de la técnica de transformación de variables de Telles y la cuadratura de Gauss adaptativo para mejorar la precisión de la integración y para disminuir el tiempo de cálculo. La selección de parámetros para el algoritmo depende de la relación entre la distancia desde el punto de colocación al elemento de integración y una longitud de referencia del elemento. Como ejemplo, el algoritmo propuesto se aplica a una placa sometida a carga uniaxial y a un cilindro tubular a presión interna, ambos de pared delgada. Los resultados obtenidos están en concordancia con los resultados teóricos y la reducción de los tiempos de integración es significativa.

----------*Palabras clave:* MEC, placas, carcasas, integración numérica, transformación polinómica

Introduction

Thin-walled plates and shells are very important due to their wide use in industry, i.e. pressure vessels and piping systems. In this type of structures the thickness is small in comparison with the other dimensions and their design implies the requirement of an accurate stress analysis that generally, due to the complexity of the system evaluated, requires the use of numerical methods such as the Finite Element Method (FEM) or the Boundary Element Method (BEM).

The FEM is amply used as a numerical tool for engineering analysis, although the BEM has also been widely used in recent years as an effective alternative. The attraction of the BEM is mainly attributed to the fact that it only requires discretization of the solid boundary converting a three- dimensional problem into a two-dimensional problem, which allows easier meshing (smaller number of elements and nodes) and requires less data preparation time. Also, this dimensionality reduction allows a lower processing time than the FEM, which uses domain discretization generating a much larger system of equations [1]. The BEM allows a very accurate stress analysis inside the domain of the solid because no further approximation for the solution at interior points is imposed [2].

The stress analysis of plates can be carried out using two theories: Kirchhoff, the classic theory for thin plates, and Reissner, used for the analysis of shear deformable plates [3]. Another basic approach for treating plate problems is 3D numerical modelling based on the theory of elasticity [4], because of its solid theoretical basis.

The application of the BEM for thin-walled structures implies that collocation points and

integration elements are often very close, making the kernel of the integrations nearly singular and requiring the use of special numerical integration techniques. The BEM is not convenient for thin-walled elements due to the inaccuracy of the results [2]. However, the conventional formulation of the BEM for 3D elasticity could be applied to thin-walled elements if the near–singular integrals are correctly treated [5]. Usually, the FEM also presents several problems when applied to the analysis of thin-walled structures, because of some difficulties arising from the meshing process [5].

The regular integrals in the BEM are usually computed using standard Gaussian quadrature. However, when the source point is close to the element evaluated, but does not belong to the element, the integrals are normally computed using a very large number of Gauss points, generating large requirements of computation time and not guaranteeing the accuracy of the results. For that reason, several techniques have been developed to treat the near-singular integrals arising from thin-walled BEM applications. The most common techniques are: 1) Element subdivision using the transformation introduced by [6]; 2) Element co-ordinate transformation in order to concentrate Gauss points toward the source point projection, that include polynomial transformation [7, 8], *sinh* transformation [9-11], sigmoidal transformation [11, 12], and exponential transformation [13]; 3) Transformation into line integrals and weakly singular integrals [5, 14, 15]; 4) Semi-analytical integration based on series expansion [16, 17]; and 5) Distance transformation for damping-out the near singularity of the kernels [12, 13, 18-20]. Analytical formulations have also been applied to solve near-singular integrals for two-dimensional problems, using integration by parts for straight elements and subdivision into sub-parametric elements for curved elements [21].

Computational algorithms have also been developed to solve the near singularity problem by combining techniques in order to make methods more robust [22], such as the combination of triangular polar co-ordinate transformation introduced by [23] and third degree polynomial co-ordinate transformation proposed by [7]; the combination of Telles' transformation with an adaptive Gauss method [24]; and distance transformation in combination with element subdivision [25].

On the other hand, the thin-walled shell problem is itself a complicated problem, which can be solved using the displacement boundary integral equation in its standard formulation, modelling separately the two surfaces [5]. BEM formulations for the thin-walled shell problem have also been derived by [26] and [27], who specifically treated shell structures based on the formulation proposed by [5].

The aim of this study is to present an efficient algorithm for near–singular integration of boundary element integrals applied to three–dimensional thin-walled structures (plates and shells). The new algorithm uses a combination of an adaptive Gaussian quadrature method for regular integrals and a transformation of variables technique for nearly-singular integrals. The results of validation tests of the algorithm against theoretical calculations and their comparison to results obtained with another algorithm based on a subdivision technique are also presented.

The Boundary Element Method

The Navier equation for the theory of linear elasticity, in the absence of body forces, can be written in tensor notation as indicated in Eq. (1):

$$\left(\frac{1}{1-2\nu}\right)u_{j,ji} + u_{i,jj} = 0 \qquad (1)$$

for $i,j = 1,2,3$, where u is the displacement vector and ν is the Poisson ratio.

Using the fundamental solutions obtained by Lord Kelvin to solve Eq. (1) and applying Betti's reciprocal theorem, the Boundary Integral Equation (BIE) for elastostatic problems, known as Somigliana's Identity for displacements, which is shown in Eq. (2) [1]:

$$u_i(p)=\int_S U_{ij}(p,Q)\,t_j(Q)dS-\int_S T_{ij}(p,Q)\,u_j(Q)\,dS \quad (2)$$

where p is the collocation point, Q is a generic boundary point, and U_{ij} and T_{ij} are the fundamental solutions in three dimensions for displacement (Eq. (3)) and tractions (Eq. (4)), respectively.

$$U_{ij}(p,Q)=\frac{1}{16\pi\mu(1-\nu)r}\left[(3-4\nu)\delta_{ij}+r_{,i}\,r_{,j}\right] \quad (3)$$

$$T_{ij}(p,Q)=-\frac{1}{8\pi(1-\nu)r^2}\left\{\frac{\partial r}{\partial n}\left[(1-2\nu)\delta_{ij}+3r_{,i}\,r_{,j}\right]-(1-2\nu)(r_{,i}n_j-r_{,j}n_i)\right\} \quad (4)$$

where r is the distance between p and Q, μ is the shear modulus of elasticity and n is the outward normal at point Q.

Taking the collocation point p to become a point P on the boundary, Eq. (2) can be expressed in the form indicated in Eq. (5):

$$C_{ij}(P)\,u_j(P)+\int_S T_{ij}(P,Q)\,u_j(Q)\,dS=\int_S U_{ij}(P,Q)\,t_j(Q)\;dS \quad (5)$$

where $C_{ij}(P)$ is the free term coefficient matrix arising from the jump of the Cauchy principal value (CPV) integral.

The next step is the use of a parametric representation applied to the boundary coordinates (x_j), displacements (u_j) and tractions (t_j) in Eq. (5), using the interpolation functions indicated in Eq. (6) [2]:

$$x_j=\sum_{\alpha=1}^{m}N_\alpha(\xi_1,\xi_2)\,x_j^\alpha;\quad u_j=\sum_{\alpha=1}^{m}N_\alpha(\xi_1,\xi_2)\,u_j^\alpha;\quad t_j=\sum_{\alpha=1}^{m}N_\alpha(\xi_1,\xi_2)\,t_j^\alpha\quad -1\le\xi_1,\xi_2\le 1 \quad (6)$$

where $N\alpha$ (ξ_1, ξ_2) are the interpolation functions at node α. This transformation is equivalent to converting the boundary elements into a square in local coordinates in the ξ_1,ξ_2 plane.

The discretized form of Eq. (5) using the above approximations is presented in Eq. (7):

$$C_{ij}(P)u_j(P)+\sum_{n=1}^{Ne}\sum_{a=1}^{m}V_{ij}^{na}u_j^{na}=\sum_{n=1}^{Ne}\sum_{a=1}^{m}W_{ij}^{na}t_j^{na} \quad (7)$$

where V_{ij}^{na} and W_{ij}^{na} are computed using Eq. (8) and Eq. (9), respectively.

$$V_{ij}^{na}=\int_{-1}^{1}\int_{-1}^{1}N_a(\xi_1,\xi_2)T_{ij}\left[P,Q(\xi_1,\xi_2)\right]J^n(\xi_1,\xi_2)\,d\xi_1\,d\xi_2 \quad (8)$$

$$W_{ij}^{na}=\int_{-1}^{1}\int_{-1}^{1}N_a(\xi_1,\xi_2)U_{ij}\left[P,Q(\xi_1,\xi_2)\right]J^n(\xi_1,\xi_2)\,d\xi_1\,d\xi_2 \quad (9)$$

J^n is the Jacobian of the transformation.

Equation (7) can be expressed in matrix form as: *[H]{u} = [G]{t}*. The matrices *[H]* and *[G]* contain values obtained by Equations (8) and (9), respectively. The next step is the application of known mixed boundary conditions (displacements and tractions), generating the system of equations *[A]{X}= [F]*, which solution produces the initially unknown displacement and traction variables contained in vector *{X}*.

Strongly, weakly and nearly singular integrals

The integral on the left side of Eq. (5) is strongly singular while the integral on the right side of Eq. (5) is weakly singular. The evaluation of strongly and weakly singular integrals has been a central topic in the application of BEM for plate problems, and several proposed techniques are discussed in [28]. In this work, the strongly singular integrals (CPV integrals) have been calculated by applying rigid-body displacements of the whole body in the directions of the coordinate axes [29], while the weakly singular integrals are regularised through the coordinate transformation [30] indicated in Eq. (6), which allows the use of regular integration techniques [2].

However, when the collocation point (P) is close to the element under evaluation, but does not

belong to it (*r* is small, but not zero), the integrals in Eq. (5) are nearly singular. The reason is due to the behaviour of the *1/r* and $1/r^2$ terms in the kernels U_{ij} and T_{ij}, which cause sharp variations of the integrands.

As mentioned in the Introduction, several methods can be used to deal with this problem. Gaussian quadrature, element subdivision and Telles' transformation are used in this work based on the ratio *r/l* (*l* is the element length), which is very useful for defining the most appropriate type of scheme to evaluate near–singular integrals [24].

Gaussian Quadrature

Gaussian quadrature is based on the approximation indicated in Eq. (10) [1]:

$$\int_{-1}^{1}\int_{-1}^{1} f(\xi_1,\xi_2)\,d\xi_1\,d\xi_2 = \sum_{S1=1}^{S_1}\sum_{S2=1}^{S_2} A_{S_1}\,A_{S_2} f(\xi_{S_1},\xi_{S_2}) \quad (10)$$

where S_1 and S_2 are the number of Gauss points, A_{S1} and A_{S2} are their weights, ξ_{S1} and ξ_{S2} are the abscissas of the Gauss points.

Element Subdivision

This method implies that the integration element is divided into *M* cells (number of subdivisions in the ξ_1 direction) × *L* cells (number of subdivisions in the ξ_2 direction) [1], and Gauss quadrature is used for evaluating the integrals in each cell. The integrals can be written as presented in Eq. (11):

$$\int_{-1}^{1}\int_{-1}^{1} f(\xi_1,\xi_2)\,d\xi_1\,d\xi_2 = \frac{1}{ML}\sum_{m=1}^{M}\sum_{l=1}^{L}\sum_{s1=1}^{S_1}\sum_{s2=1}^{S_2} A_{S_1}\,A_{S_2} f(\bar{\xi}_{S_1},\bar{\xi}_{S_2})$$

$$\xi_{S_1} = \frac{1}{M}\left[M-2m+1+\xi_{S_1}\right];$$

$$\bar{\xi}_{S_2} = \frac{1}{L}\left[L-2l+1+\xi_{S_2}\right] \quad (11)$$

The element subdivision method is the most popular to evaluate near–singular integrals, but due to the Gaussian quadrature it uses to integrate each of the (*M x L*) generated cells, it requires a very long computer time [14].

Telles' Transformation

Telles' polynomial transformation uses a third–degree change of variables, as indicated in Equations (12) and (13):

$$\xi_1 = a_1\eta_1^3 + b_1\eta_1^2 + c_1\eta_1 + d_1 \quad (12)$$

$$\xi_2 = a_2\eta_2^3 + b_2\eta_2^2 + c_2\eta_2 + d_2 \quad (13)$$

These polynomials transform the V_{ij}^{na} and W_{ij}^{na} integrals in Equations (8) and (9) into Equations (14) and (15):

$$V_{ij}^{na} = \int_{-1}^{1}\int_{-1}^{1} N_a(\eta_1,\eta_2)T_{ij}[x',x(\eta_1,\eta_2)]J^n(\xi_1,\xi_2)J^n(\eta_1,\eta_2)\,d\eta_1\,d\eta_2 \quad (14)$$

$$W_{ij}^{na} = \int_{-1}^{1}\int_{-1}^{1} N_a(\eta_1,\eta_2)U_{ij}[x',x(\eta_1,\eta_2)]J^n(\xi_1,\xi_2)J^n(\eta_1,\eta_2)\,d\eta_1\,d\eta_2 \quad (15)$$

This transformation causes the Gauss points to bunch together towards the collocation point when this point is located outside and close to the element plane.

Telles' transformation solves quasi–singularities in the integrals for small values of *r*, is adaptive and more accurate than the subdivision method [7].

New Algorithm

In this work, two algorithms to evaluate near–singular integrals present in the BEM are compared. Algorithm 1 (original) consists in the application of the element subdivision technique for $r/l \leq 2.0$, in combination with non-adaptive Gauss quadrature for $r/l > 2.0$. Algorithm 2 (proposed) uses a combination between Telles' transformation using third-degree polynomials with an adaptive Gaussian quadrature, whose configuration is presented in table 1.

Table 1 Algorithm 2 (Proposed) – Configuration

A. Start regular integration of kernels	
i = (Integer part of $0.3\ l/r$)+1.0	Determine i – requirement of adaptive algorithm r: distance between P and node Q of the element in evaluation *l: smallest value between side length and element diagonal length*
If $i = 1$. Kernel integration using Gauss	Determine the Gauss points as a function of r/l ratio (See table 2)
If $i > 1$. Telles' transformation using 16 Gauss points.	
B. Start Telles' transformation	
Determine node coordinates $\overline{\xi}$	$\overline{\xi}$: Node closest to P
Determine minimum distance r between P and node $\overline{\xi}$	
Select equation of $\overline{r}$ to use	
Determine $\overline{\eta}$ and coefficients a, b, c and d	
Determine third-degree polynomial and Jacobian using Gauss coordinates	Eq. (12) and Eq. (13), and its derivatives
C. Integration of kernels in the BEM	***Eq. (14) and Eq. (15)***

The conditions included in the new algorithm in order to reach the adaptability to a thin-walled problem are shown in table 2. The number of Gauss points increases when the r/l ratio is reduced until r/l=0.3, the value where Telles' transformation starts being used by the algorithm.

Table 2 Algorithm 2 (Proposed) – Basis

Condition	*Integration Method*
$r/l > 4.0$	Gaussian quadrature 2 x 2
$1.38 < r/l \leq 4.0$	Gaussian quadrature 4 x 4
$1.0 < r/l \leq 1.38$	Gaussian quadrature 8 x 8
$0.48 < r/l \leq 1.0$	Gaussian quadrature 12 x 12
$0.3 < r/l \leq 0.48$	Gaussian quadrature 16 x 16
$r/l \leq 0.3$	Telles' transformation

Methodology

Plate

The algorithms were tested on a model of a thin-walled plate, with dimensions 3.0 m length, 1.0 m width and 0.01 m thickness, in the absence of body forces. The plate is clamped at one edge and subject to a distributed axial load of 10 kN on the free edge, E = 200 GPa and ν = 0.3. The plate boundary was discretized using eight-node quadrilateral elements in four different meshes, shown in table 3. This table also shows the minimum r/l ratio reached in each case.

Table 3 Thin-walled Plate: Meshes used

Mesh Case	*Elements*	*Nodes*	*Discretization Step*	*Minimum r/l*
1	86	260	1	0.015
2	128	386	5/6	0.020
3	190	572	2/3	0.025
4	334	1004	1/2	0.033
5	466	1400	2/5	0.040

Four different cases were used to calculate stresses and strains in the plate: Algorithm 1-4 Gauss points, Algorithm 1-8 Gauss points, Algorithm 1-16 Gauss points, and Algorithm 2 (proposed) – Adaptive. The stress and strain results were compared to theoretical calculations based on the state of stress and strain in a plate (transversal area *A*) loaded with an axial force *Fz* [31], and the L^1 relative error norms given by Eq. (16):

$$L^1 \text{ error} = \frac{1}{m}\sum_{i=1}^{m}\frac{\left\| u_{e(i)} - u_{c(i)} \right\|}{\left\| u_{e(i)} \right\|} \qquad (16)$$

where *m* is the number of nodes whose values (stress or strain) were obtained, u_e is the exact value and u_c is calculated by the BEM.

Cylindrical Shell

Thin-walled cylindrical shells are evaluated for five different R_i/t relationships in order to assess the impact of the thinness of the wall on the accuracy of the BEM results. Only a quarter of the cylinder is modelled to take advantage of the cylinder´s double symmetry. The cylinder dimensions are R_i=500 mm, width = 15 mm and wall thickness required to match the R_i/t ratios considered (see Table 4).

The boundary conditions used for the modelling are: 1) zero displacement in perpendicular direction to both tangential walls of the quarter of cylinder, and 2) the inside wall is loaded with an internal pressure of 1.0 MPa. The material used has a linear elastic behavior with E = 200 GPa and ν = 0.3.

Table 4 Cases evaluated for Cylindrical Shell

R_i/t	t (mm)	Elements	Nodes	Minimumr/l
10.0	50.0	58	176	0.122
40.0	12.5	54	164	0.101
50.0	10.0	54	164	0.081
62.5	8.0	54	164	0.065
75.0	6.5	54	164	0.054

The stress and strain results were compared to theoretical calculations based on the state of stress and strain (directions circumferential and radial) in a linear elastic cylindrical shell subject to internal pressure only [31], and the L^1 relative error norms given by Eq. (16).

Similarly to the plate cases, the shell boundary was discretized using eight-node quadrilateral elements for five different Ri/t relationships, keeping a similar number of elements in order to test the *r/l* ratio. In table 4, the data used for meshing the boundary in each case is presented, highlighting the minimum *r/l* reached for each case.

Later, a R_i/t=75 cylinder using different element sizes ranging from 60mm to 6 mm was modelled in order to determine the influence of the *r/l* ratio and the convergence of each algorithm. The data used for these cases are shown in table 5.

Table 5 Cases evaluated for Ri/t = 75 Cylinder

Element Size (mm)	Number of Elements	Number of Nodes	Discretization Step	Minimum r/l
60	54	164	1	0.0545
48	70	212	4/5	0.0712
36	90	272	3/5	0.0922
24	134	404	2/5	0.1383
12	266	800	1/5	0.2223
6	534	1604	1/10	0.2700

All the tests were carried out using a BEM code in the Fortran language, which was updated and modified using a Visual Fortran compiler edition 6.0 and ran in a Pentium (R) Dual-Core CPU E5200 with 2.50GHz processor clock with 3.00 GBytesRAM. The computing time of the algorithms was measured through the insertion of the function FDATE at the beginning and at the end of the integration process to the respective Fortran code.

Results

Plate

The average maximum principal stress obtained with five different meshes (see Table 3) using two algorithms and its comparison to the analytical solution are shown in figure 1.

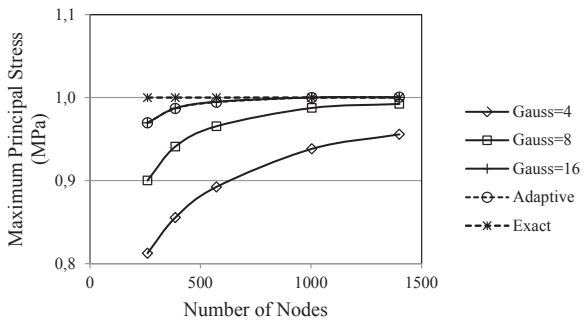

Figure 1 Average Maximum Principal Stress - Plate

The new algorithm (Adaptive) is more accurate than algorithm 1 (Original) using 4 and 8 Gauss integration points. For 16 Gauss points, the results obtained by algorithm 1 are similar to those found by the new one.

Figure 2 shows the average maximum principal strain obtained at the free edge. Similarly to the stress results, algorithm 2 is more accurate than algorithm 1 with 4 and 8 Gauss integration points. For 16 Gauss points, the results are similar to the algorithm proposed.

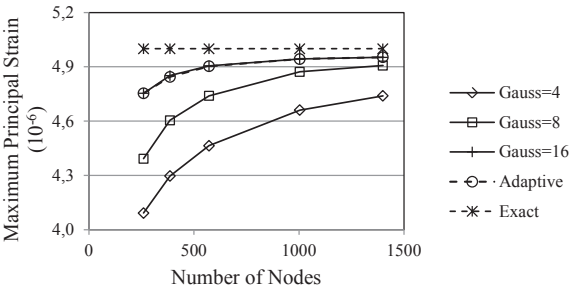

Figure 2 Maximum Principal Strain Values – Plate´s Free Edge

The convergence, considering a tolerance of 0.01, is reached at 572 nodes for the Adaptive and algorithm 1 with 16 points; for 8 points, convergence is achieved at 1400 nodes, while for 4 Gauss points convergence is not reached.

Figure 3 presents the L^1 relative error norms for the maximum principal strain results determined in the free edge as a function of the discretization step used for modelling the thin-walled plate.

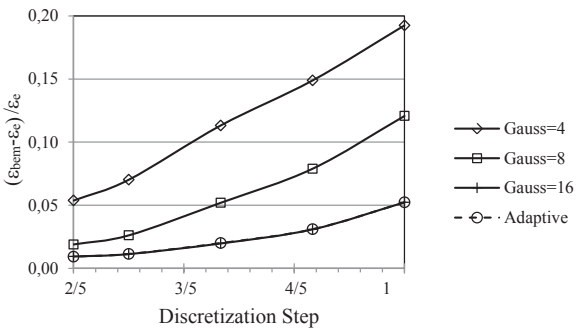

Figure 3 L^1 Relative error norms for Maximum Principal Strain Results - Case: Plate

The convergence to the exact solution for the new algorithm and 16 Gauss points have a slope of 2.9, for 8 Gauss points the slope is 3.1, the highest, and the slope for 4 points is the lesser, 2.1. The behavior of the convergence rate for the stress calculations is similar.

In reference to the computation time required for evaluating the singular, quasi – singular and regular integrals present in the BEM, figure 4

shows that the new algorithm required the least time of all, while the algorithm with 16 Gauss points required the most integration time.

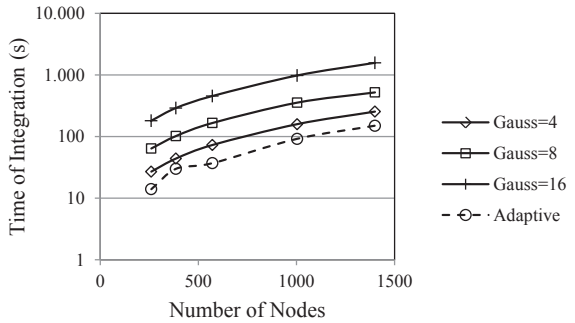

Figure 4 Time of Integration – Case: Plate

The original algorithm could generate similarly good results for 16 Gauss integration points but using an integration time around 1000% greater than the new adaptive algorithm.

Cylindrical Shell

Impact of Ri/t

Figure 5 shows internal hoop stresses along the cylinder inner wall for typical thin-walled radius - thickness ratios (R_i/t), using the same two algorithms for calculating quasi–singular integrals that were applied to the thin-walled plate.

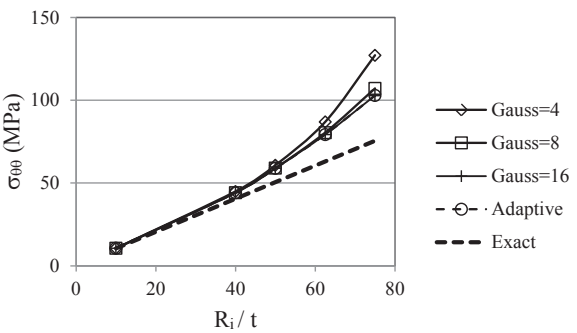

Figure 5 Hoop Stress along cylinder inner wall

The circumferential strain$\varepsilon_{\theta\theta}$, which by definition is the ratio between the change in length of the internal radius ΔR_i and R_i [31], is presented in figure 6.

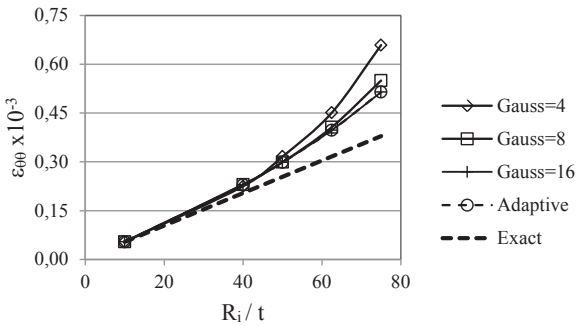

Figure 6 Circumferential Strain along cylinder inner wall

In both figures, it can be noted that the differences between the numerical results obtained by the BEM and the exact values increase as the cylinder gets thinner, that is, when the R_i/t ratio increases, demonstrating the problem that the BEM has when modelling thin-walled shell-like structures. The accuracy for high values of R_i/t, however, can be restored by further increasing the number of Gauss points.

The L^1 relative error norms for the circumferential strain between the BEM results and the exact solution are presented in figure 7.

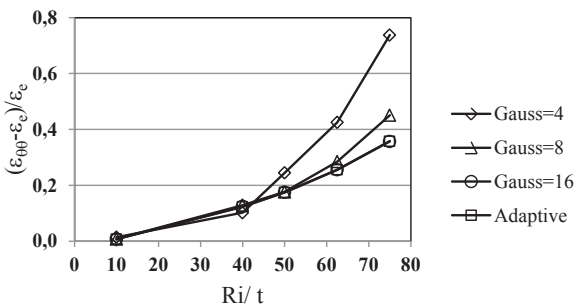

Figure 7 L^1 Relative error norms for Circumferential Strain along cylinder inner wall

For R_i/t= 10, the known limit between thin and thick walled, the results for both algorithms are similar and in good agreement with the analytical solution. When increasing the R_i/t ratio, the

relative error and the difference between the algorithms grow, except for 16 Gauss points. These results are consistent with the minimum *r/l* relationship related to each R_i/t (see Table 4). The lower *r/l* is, the higher the differences between the results obtained by the algorithms, with the proposed Adaptive algorithm always producing better results.

Although the original algorithm with 16 Gauss points and the proposed one show similar accuracies, the integration times for 16 points are much greater than for the proposed one. The adaptive algorithm requires the lowest integration time of them all (see Table 6).

Table 6 Time of Integration (s)

R_i/t	Gauss=4	Gauss=8	Gauss=16	Adaptive
10.0	11	22	65	8
40.0	14	31	96	8
50.0	14	33	109	9
62.5	18	38	115	8
75.0	18	38	116	9

Figure 8 shows the internal hoop stresses for R_i/t=75 and different values of the minimum *r/l* ratio, related to the number of elements (see table 5). As the minimum *r/l* is reduced, the BEM loses accuracy in all cases, with the new algorithm always providing the best accuracy.

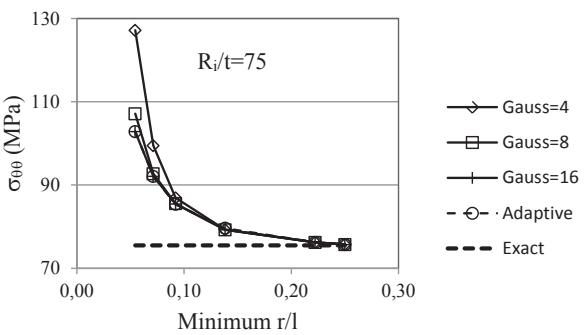

Figure 8 Hoop Stress along cylinder inner wall vs. Minimum r/l – Ri/t=75

Impact of r/l

Figure 9 presents the L^1 relative error norms for the circumferential strain in the cylinder inner wall as a function of the minimum *r/l* generated for modelling the thin-walled shell-like structure.

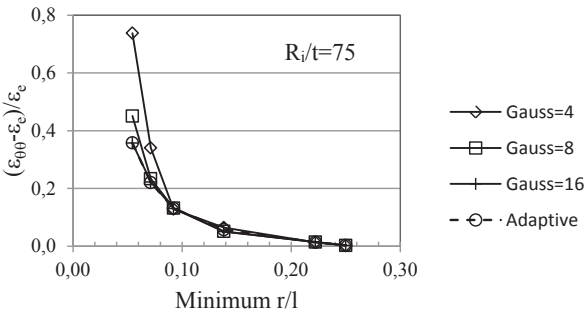

Figure 9 L^1 Relative error norms for Circumferential Strain along cylinder inner wall

For *r/l* ratio values greater than 0.09, all algorithms generated similar results, but for lesser *r/l* values the BEM loses accuracy. The accuracy for low values of *r/l*, however, can be restored by further increasing the number of Gauss points. In reference to the computation time required for evaluating the integrals present in the BEM, figure 10 shows that the new algorithm required the least time of all, while the algorithm with 16 Gauss points required the most integration time.

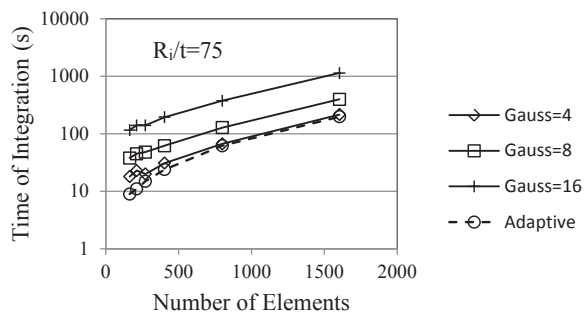

Figure 10 Time of Integration – Case: Cylindrical shell - R_i/t = 75

The original algorithm could generate similarly good results for 16 Gauss integration points but

using an integration time around 500% greater than the new algorithm.

Conclusion

A new algorithm to evaluate near–singular integrals appearing in the application of the BEM to thin walled structures (plate and cylindrical shell) has been presented. This new algorithm, which uses a combination of Telles' transformation of variable technique and adaptive Gaussian Quadrature, generates stress and strain values in good agreement with theoretical results, and more accurate than the results given by an existing algorithm, except for 16 Gauss integration points. However, the proposed algorithm requires much less computer time than the original algorithm.

Acknowledgment

The work reported in this article was carried out at Brunel University, UK. Marco Gonzalez acknowledges the support of the αlfa – ELBENet Project, Marie Curie Programme of the European Commission, and the help provided by Simon Bolivar University, Caracas, Venezuela.

References

1. L. Wrobel, M. Aliabadi. *The Boundary Element Method.* 1st ed. Ed. John Wiley & Sons. New York, USA. 2002. pp. 491-523.

2. A. Becker. *Boundary Element Method in Engineering: A Complete Course*. 1st ed. Ed. McGraw Hill. London, UK. 1992. pp. 1-14.

3. A. Zehnderand, M. Viz. "Fracture mechanics of thin plates and shells under combined membrane, bending and twisting loads". *Applied Mechanics Reviews*. Vol. 58. 2005. pp. 37-48.

4. C. Providakis, D. Beskos. "Dynamic analysis of plates by boundary elements". *Applied Mechanics Reviews.* Vol. 52. 1999. pp. 213-236.

5. Y. Liu. "Analysis of shell-like structures by the Boundary Element Method based on 3-D elasticity: formulation and verification". *International Journal for Numerical Methods in Engineering*. Vol. 41. 1998. pp. 541-558.

6. J. Lachat, J. Watson. "Effective numerical treatment of Boundary Integral Equations: A formulation for three-dimensional elastostatics". *International Journal for Numerical Methods in Engineering*. Vol. 10. 1976. pp. 991-1005.

7. J. Telles. "A self-adaptive co-ordinate transformation for efficient numerical evaluation of general boundary element integrals". *International Journal for Numerical Methods in Engineering*. Vol. 24. 1987. pp. 959-973.

8. W. Ye. "A new transformation technique for evaluating nearly singular integrals". *Computational Mechanics.* Vol. 42. 2008. pp. 457-466.

9. Y. Gu, W. Chen, C. Zhang. "The sinh transformation for evaluating nearly singular boundary element integrals over high-order geometry elements". *Engineering Analysis with Boundary Elements*. Vol. 37. 2013. pp. 301-308.

10. P. Johnston, B. Johnston, D. Elliott. "Using the iterated sinh transformation to evaluate two dimensional nearly singular boundary element integrals". *Engineering Analysis with Boundary Elements*. Vol. 37. 2013. pp. 708-718.

11. B. Johnston, P. Johnston, D. Elliott. "A new method for the numerical evaluation of nearly singular integrals on triangular elements in the 3D boundary element method". *Journal of Computational and Applied Mathematics*. Vol. 245. 2013. pp. 148-161.

12. J. Rong, L. Wen, J. Xiao. "Efficiency improvement of the polar coordinate transformation for evaluating BEM singular integrals on curved elements". *Engineering Analysis with Boundary Elements*. Vol. 38. 2014. pp. 83-93.

13. Y. Zhang, X. Li, V. Sladek, J. Sladek, X. Gao. "Computation of nearly singular integrals in 3D BEM". *Engineering Analysis with Boundary Elements*. Vol. 48. 2014. pp. 32-42.

14. Y. Liu, D. Zhang, F. Rizzo. *Nearly singular and hypersingular integrals in the Boundary Element Method*. Boundary Elements XV, Proceedings of the 15th Int. Conf. on Boundary Elements. Massachusetts, USA. 1993. pp. 453-468.

15. S. Mukherjee, M. Chati, X. Shi. "Evaluation of nearly singular integrals in boundary element contour and node methods for three-dimensional linear elasticity". *International Journal of Solids and Structures*. Vol. 37. 2000. pp. 7633-7654.

16. Z. Niu, W. Wendland, X. Wang, H. Zhou. "A semi-analytical algorithm for the evaluation of the nearly

singular integrals in three-dimensional boundary element methods". *Computer Methods in Applied Mechanics and Engineering*. Vol. 194. 2005. pp. 1057-1074.

17. H. Hosseinzadeh, M. Dehghan. "A simple and accurate scheme based on complex space C to calculate boundary integrals of 2D boundary elements method". *Computers & Mathematics with Applications*. Vol. 68. 2014. pp. 531-542.

18. H. Ma, N. Kamiya. "A general algorithm for the numerical evaluation of nearly singular boundary integrals of various orders for two- and three-dimensional elasticity". *Computational Mechanics*. Vol. 29. 2002. pp. 277-288.

19. G. Xie, J. Zhang, X. Qin, G. Li. "New variable transformations for evaluating nearly singular integrals in 2D boundary element method". *Engineering Analysis with Boundary Elements*. Vol. 35. 2011. pp. 811-817.

20. G. Xie, F. Zhou, J. Zhang, X. Zheng, C. Huang. "New variable transformations for evaluating nearly singular integrals in 3D boundary element method". *Engineering Analysis with Boundary Elements*. Vol. 37. 2013. pp. 1169-1178

21. Z. Niu, C. Cheng, H. Zhou, Z. Hu. "Analytic formulations for calculating nearly singular integrals in two-dimensional BEM". *Engineering Analysis with Boundary Elements*. Vol. 31. 2007. pp. 949-964.

22. F. Araújo, K. Silva, J. Telles. "Generic domain decomposition and iterative solvers for 3D BEM problems". *International Journal for Numerical Methods in Engineering*. Vol. 68. 2006. pp. 448-472.

23. H. Li, G. Han, H. Mang. "A new method for evaluating for evaluating singular integrals in stress analysis of solids by the direct boundary element method". *International Journal for Numerical Methods in Engineering*. Vol. 21. 1985. pp. 2071–2098.

24. R. Rigby. *Boundary Element Analysis of Cracks in Aerospace Structures*. PhD Thesis, University of Portsmouth. Portsmouth, UK. 1995. pp. 25-32

25. X. Qin, J. Zhang, G. Xie, F. Zhou, G. Li. "A general algorithm for the numerical evaluation of nearly singular integrals on 3D boundary element". *Journal of Computational and Applied Mathematics*. Vol. 235. 2011. pp. 4174-4186.

26. S. Mukherjee. "Integral equation formulation for thin shells—revisited". *Engineering Analysis with Boundary Elements*. Vol. 31. 2007. pp. 539-546.

27. F. Araújo, K. Silva, J. Telles. "Application of a generic domain-decomposition strategy to solve shell-like problems through 3D BE models". *Communications in Numerical Methods in Engineering*. Vol. 23. 2007. pp. 771-785.

28. A. Frangi, M. Guiggiani. "Boundary element analysis of Kirchhoff plates with direct evaluation of hypersingular integrals". *International Journal for Numerical Methods in Engineering*. Vol. 46. 1999. pp. 1845-1863.

29. M. Guiggiani. "The evaluation of Cauchy principal value integrals in the boundary element method – A review". *Mathematical and Computer Modelling*. Vol. 15. 1991. pp. 175-184.

30. D. Beskos. "Boundary element methods in dynamic analysis: Part II (1986-1996)". *Applied Mechanics Reviews*. Vol. 50. 1997. pp. 149-197.

31. N. Dowling. *Mechanical Behavior of Materials. Engineering Methods for Deformation, Fracture, and Fatigue*. 3rd ed. Ed. Prentice Hall. New Jersey, USA. 2007. pp. 785-786.